

Development of a displacement-reactivity feedback model for dynamic behavior simulation in fast burst reactor

Jiang-Meng Wang^{1,2} · Hui Gao^{1,2} · Qi-Lin Xie^{1,2} · Xiao-Qiang Fan^{1,2} · Da-Zhi Qian^{1,2}

Received: 30 September 2018 / Revised: 17 December 2018 / Accepted: 22 December 2018 / Published online: 13 April 2019
© China Science Publishing & Media Ltd. (Science Press), Shanghai Institute of Applied Physics, the Chinese Academy of Sciences, Chinese Nuclear Society and Springer Nature Singapore Pte Ltd. 2019

Abstract In this study, a displacement-reactivity feedback model, which can directly represent the inherent “thermal expansion extinction effect” of fast burst reactors (FBRs), was developed with the aid of the static neutron transport component of the FBR-MPC code. Dynamic behaviors of bursts in the Godiva I reactor were simulated by coupling the simplified multiphysics models consisting of the point kinetic equations for neutronics, adiabatic equation for temperature, and thermoelastic equations for displacement/stress with the developed model. The results were compared with the corresponding experimental data and those obtained using the traditional fission yield (temperature rise)-reactivity feedback models. It was found that the developed model can provide good results for the bursts with no or a small inertia effect. For the bursts with a prominent inertia effect, the smaller burst width and asymmetric distribution of the fission rate curve, noticed in the experiments but not evident using the traditional models, can be reproduced. In addition, the realistic oscillations in reactivity and fission rate caused by the core vibration, as well as the deeper sub-prompt criticality in the plateau following the burst, can be observed. Therefore, the developed displacement-reactivity feedback model can be

expected to be an effective tool for calculating the dynamic behaviors of bursts.

Keywords Displacement-reactivity feedback model · Prompt supercritical · Coupled calculation · Fast burst reactor

1 Introduction

In a fast burst reactor (FBR), to trigger a burst, one first inserts a certain reactivity in the core to transit the system from sub-delayed-critical to super-prompt-critical. Thereafter, by injecting source neutrons, the fission rate quickly increases after the first persistent fission chain is established. The released fission energy results in the temperature rise and hence core expansion, which in turn leads to the decrease in reactivity. As a result, the increasing velocity of the fission rate gradually decreases to zero at the time of its peak, and the fission rate decreases to a low-amplitude plateau, representing the thermal expansion extinction effect [1]. Particularly, when the core expansion cannot accommodate the temperature rise (i.e., the core does not simultaneously expand to the same status of static expansion caused by temperature rise), the core appears compressed. This compression later produces vibrational displacements and potentially large dynamic stresses, i.e., the inertia effect [2, 3].

The dynamic behavior of the burst is highly complicated because of its short duration (usually less than ~ 100 ms) and intense variations in the coupled neutronics–temperature–thermoelastics fields. To obtain an accurate picture of this dynamic behavior, a coupled calculation based on three-dimensional (3D) time-dependent multiphysics

This work was supported by a General Financial Grant from the China Postdoctoral Science Foundation (No. 2017M623313XB) and Key Laboratory of Neutron Physics, CAEP (No. 2018BA02).

✉ Da-Zhi Qian
qdz1968@vip.sina.com

¹ Key Laboratory of Neutron Physics, China Academy of Engineering Physics, Mianyang 621900, China

² Institute of Nuclear Physics and Chemistry, China Academy of Engineering Physics, Mianyang 621900, China

models requiring neutron transport equations for neutronics, a heat conduction equation for temperature, and thermoelastic equations for displacement/stress needs to be developed. In recent years, increasing efforts have been made to develop coupled codes using accurate multiphysics models, such as the enhanced MRKJ code for a one-dimensional (1D) spherical case [2], the OpenFOAM-based discrete ordinates solver for coupled neutron transport/thermomechanical calculations [4], and our 3D coupled multiphysics FEM (finite element method) code FBR-MPC [5].

However, as observed in previous works [1, 5], for small FBRs with a simple core structure such as the unreflected spherical Godiva I reactor, the point kinetic approximation is sufficiently accurate for neutronics. Because the burst duration can be neglected as compared to the heat balance time, the adiabatic approximation is also applicable for temperature calculation. Thus, in such cases the burst dynamic behavior can be well described using the simplified multiphysical models consisting of the point kinetic equations for neutronics, the adiabatic equation for temperature, and the thermoelastic equation for displacement/stress, similar to previous works [1, 2]. However, for bursts with the inertia effect, the realistic fission rate oscillation caused by the core vibration, noticed in earlier experiments [6, 7] and reproduced in our previous work [5], was not touched upon in early theoretical studies. The main reason is that the applied traditional fission yield (temperature rise)-reactivity feedback models were established upon the assumption that the reactivity change is proportional to the fission yield (or the equivalent temperature rise), and thus, the reactivity monotonically decreases in the burst [1, 7, 8].

To overcome the disadvantage of the traditional fission yield (temperature rise)-reactivity feedback model and directly represent the inherent “thermal expansion extinction effect” of the FBR, a natural thought is to establish the relation between the reactivity change and core expansion (or more specifically the displacement). This can be achieved considering the expression of the spatial distribution of the displacement at an arbitrary time in the burst as the sum of a series of orthogonal functions. If the reactivity change component for the displacement in the form of each orthogonal function can be obtained, the total reactivity change can be calculated as the sum of all its components. The coefficients of orthogonal functions are the relative weights of the corresponding reactivity change components. Therefore, several static neutron transport calculations are required to establish this displacement-reactivity feedback model. The burst dynamic behavior can be easily obtained by calculating the simplified multiphysics models using the displacement-reactivity feedback model. The preliminary advantage of this method is the high calculation efficiency as compared to the simulations

using accurate 3D coupled time- and space-dependent multiphysical models. Another benefit is that unlike cases using traditional models, predetermination of whether the inertia effect is generated prior to simulation is not required. The reactivity change components for the displacements in the form of orthogonal functions can be calculated using a deterministic neutron transport code, such as the static neutron transport component of our FBR-MPC code. The widely used Monte Carlo radiation transport codes cannot be adopted to achieve this goal because the uncertainty associated with the reactivity may be much higher than the reactivity change due to the small core expansion [9].

The main purpose of this work was to develop and verify a displacement-reactivity feedback model for FBRs. The structure of this paper is as follows. Initially, the simplified multiphysical models and numerical algorithms, together with the traditional reactivity feedback models and the main parameters of burst calculated using these models, are introduced. Next, the procedure for developing the displacement-reactivity feedback model is presented in detail. Coupled calculations using this developed model and simplified multiphysical models are then performed for various bursts in the Godiva I reactor. Finally, the results are compared to experimental data and those obtained using the traditional reactivity feedback models to verify the applicability of the developed model. Some interesting features noticed in the experiments, but not reported in early theoretical works, are also discussed.

2 Theoretical models

In the present study, the unreflected spherical homogeneous Godiva I was selected as the model reactor. It was chosen because of its simple configuration (the relation between the reactivity change and displacement can be easily determined) and the availability of numerous experimental data and theoretical results that can be used to verify the displacement-reactivity feedback model

Table 1 Main parameters for Godiva I reactor [4]

Parameters	Value
Radius (cm)	8.7407
Young's modulus (GPa)	208
Poisson ratio	0.23
Linear thermal expansion coefficient (1/K)	1.39E−5
Specific heat capacity [J/(g K)]	0.1177
Heat released per fission (J)	2.848E−11

developed. Basic parameters for the Godiva I reactor were taken from the literature [4] and are listed in Table 1.

2.1 Simplified multiphysical models for neutronics, temperature, and displacement

The literature [5] has proved the assumption used in early works [1, 2, 7, 9] that in the Godiva I reactor, the spatial distribution of the fission rate is independent from the temporal variation. In one-group isotropic scattering theory, the point kinetic approximation for neutronics can be used. The point kinetic equation for the fission rate and the balance equation for the delayed neutron precursors are as follows [10]:

$$\frac{dF(t)}{dt} = \frac{\rho(t) - \beta_{\text{eff}}}{\Lambda} F(t) + \frac{1}{v_f \Lambda} \sum_{i=1}^6 \lambda_i C_i(t), \quad (1)$$

$$\frac{dC_i(t)}{dt} = v_f \beta_{\text{eff},i} F(t) - \lambda_i C_i(t), \quad (2)$$

where ρ is the reactivity, β_{eff} is the effective delayed neutron fraction, Λ is the neutron generation time, v_f is the average number of neutrons generated per fission, λ is the decay constant, F is the fission rate, C is the precursor density, t is the time, and the subscript i is the group number of the precursors.

The burst duration is typically ignorable compared to the heat balance time such that both the heat conduction in the core and the heat exchange through the surface can be neglected, i.e., the adiabatic approximation can be applied as follows:

$$\rho_V(r, t) c_p \frac{dT(r, t)}{dt} = \varepsilon_f F(r, t), \quad (3)$$

where ρ_V is the density, c_p is the specific heat capacity, T is the temperature rise, ε_f is the average energy released per fission, and r is the location in the radial coordinate system.

With the limitation in purely elastic behavior, i.e., the operation of the FBR is under a controlled condition, the displacement in the core can be calculated using the 1D elastic wave equation as follows [10]:

$$\rho_V \frac{\partial^2 u}{\partial t^2} = (\lambda + 2\mu) \frac{\partial}{\partial r} \left[\frac{\partial u}{\partial r} + \frac{2}{r} u \right] - \alpha(3\lambda + 2\mu) \frac{\partial T}{\partial r}, \quad (4)$$

where the Lamé constants are defined as follows:

$$\lambda = \frac{\nu E}{(1 + \nu)(1 - 2\nu)}, \quad \mu = \frac{E}{2(1 + \nu)}. \quad (5)$$

Similar to the literature [9], the free boundary condition is applied on the core surface as follows:

$$(\lambda + 2\mu) \frac{\partial u_R}{\partial r} + \frac{2\lambda u_R}{R} = (3\lambda + 2\mu) \alpha T_R, \quad (6)$$

where u is the displacement, α is the linear thermal expansion coefficient, ν is the Poisson ratio, E is the Young's modulus, and R is the core radius.

2.2 Numerical algorithms

To obtain the temporal variations and/or spatial distributions of the fission rate, temperature rise, and displacement, proper numerical algorithms should be adopted to calculate Eqs. (1)–(4).

In this study, the space-dependent terms in Eqs. (1)–(4) were discretized using the finite difference method. Considering that the variation in the fission rate will result in changes in the temperature rise and displacement, which in turns leads to variations in reactivity and fission rate, the iteration calculations of fission rate, temperature rise, and displacement should be made at each time step. Therefore, the implicit scheme algorithm was applied on the time-dependent terms in Eqs. (1)–(4), i.e., the obtained fission rate from Eqs. (1) and (2) is provided as the input of adiabatic Eq. (3) to calculate the temperature rise needed in elastic wave Eq. (4). Then, the reactivity in Eqs. (1) and (2) is updated by using the developed displacement-reactivity feedback model and the displacement obtained in Eq. (4). Such an iteration carries on until reaching the convergence criterion and then moves to the coupled calculations at the next time step.

2.3 Traditional fission yield (temperature rise)-reactivity feedback models

For a burst without the inertia effect, the core expansion can accommodate the temperature rise, the distribution shape of the displacement remains the same as that in the static expansion caused by the same temperature rise, and only the magnitude of the displacement increases in proportion to the temperature rise [1, 2], i.e.,

$$u(r, t) = u_0(r) \bar{T}(t), \quad (7)$$

where u_0 is the displacement for the average temperature rise \bar{T} of 1 K in the static expansion.

For a spherical FBR, the relation between the reactivity change and displacement can be obtained by using the perturbation theory as follows:

$$\Delta\rho = 4\pi \int_0^R \rho_V u(r, t) r^2 \frac{dW(r)}{dr} dr, \quad (8)$$

where $\Delta\rho$ is the reactivity change and W is the function of perturbation coefficient.

Substituting Eq. (7) into Eq. (8) and defining the constant coefficient b_T , we obtain the following:

$$b_T = 4\pi \int_0^R \rho_V u_r(r) r^2 \frac{dW(r)}{dr} dr. \quad (9)$$

The reactivity change is thus expected in a linear relation with the temperature rise (or the equivalent fission yield) and can be calculated using the Fuchs–Hansen model [9] as follows:

$$\Delta\rho(t) = b_T \bar{T}(t) = b_f \int_0^t F(t) dt, \quad (10)$$

where b_T is the temperature-reactivity feedback coefficient and b_f is the quench coefficient defined as the absolute value of the reactivity change per fission.

When the inertia effect is generated, a lag between the core expansion and temperature rise occurs. The core appears compressed as compared to the static expansion caused by the same temperature rise, i.e., the realistic displacement $u(r, t)$ is smaller than $u_0(r) \bar{T}(t)$. Thus, the application of Eq. (10) will result in an overestimation of the reactivity decrease and underestimations of the peak fission rate and fission yield. To account for the impact of the inertia effect, a widely used method is to establish the relation between the reactivity change and fission yield with the assumption of single-frequency core vibration (only the contribution of the fundamental mode is considered and the vibrational period is also the same as the fundamental frequency) such as depicted by the following [10]:

$$\Delta\rho(t) = \frac{b_f}{1 + \alpha_0^2 \tau^2} \int_0^t F(t) dt = b'_f \int_0^t F(t) dt, \quad (11)$$

where α_0 is reciprocal of the reactor period and τ is reciprocal of the fundamental angular frequency of the core vibration.

The total reactivity can be determined as follows:

$$\rho(t) = \rho_0 - \Delta\rho(t), \quad (12)$$

where ρ_0 is the initial reactivity.

2.4 Main parameters of the burst calculated using traditional reactivity feedback models

It is known that the performance of an FBR is primarily characterized by the peak fission rate and fission yield under controlled conditions. By neglecting the delayed neutron precursors in Eq. (1) (the burst time is very short as compared to the half-life such that the precursors nearly do not decay), analytical solutions for the fission rate F and fission yield Q can be calculated using the traditional reactivity feedback models in Sect. 2.3 as follows [1, 2, 10]:

$$F(t) = \frac{2\rho_0}{b_f \Lambda} \frac{e^{\alpha_0(t-t_{\max})} (1 + \delta \alpha_0^2 \tau^2)}{(1 + e^{\alpha_0(t-t_{\max})})^2}, \quad (13)$$

$$Q(t) = \frac{2\rho_0}{b_f} \frac{(e^{\alpha_0 t} - 1)(1 + \delta \alpha_0^2 \tau^2)}{(e^{\alpha_0 t_{\max}} - 1)(e^{\alpha_0(t-t_{\max})} - 1)}, \quad (14)$$

where δ can be set as 0 or 1 when neglecting or considering the inertia effect and t_{\max} is the time of peak fission rate defined as follows:

$$t_{\max} = \frac{1}{c} \ln \frac{c + \alpha_0}{c - \alpha_0}, \quad c = \sqrt{\alpha_0^2 + 2b_f / [\Lambda(1 + \delta \alpha_0^2 \tau^2)] F(0)}. \quad (15)$$

With the adiabatic approximation, the average temperature rise can be obtained as follows:

$$\bar{T}(t) = \frac{\varepsilon_f}{mc_p} \int_0^\infty F(t) dt = \frac{\varepsilon_f}{mc_p} Q(t). \quad (16)$$

The displacement can be estimated as follows [11]:

$$u(r, t) = \frac{\varepsilon_f u_0(r)}{mc_p} Q(t) (1 + \delta \alpha_0^2 \tau^2), \quad (17)$$

where m is the material mass of the core.

By comparing Eqs. (10) and (11), it is clear that the impact of the inertia effect on the reactivity change is considered by modifying the quench coefficient b_f with a constant factor of $1/(1 + \alpha_0^2 \tau^2)$, which indicates that the fission rate/yield, temperature rise, and displacement are $(1 + \alpha_0^2 \tau^2)$ times those neglecting the inertia effect.

3 Development of a displacement-reactivity feedback model

For a burst without the inertia effect, the core expansion can accommodate the temperature rise, Eq. (7) can be applied, and the reactivity change $\Delta\rho$ has a linear relation to the displacement or the equivalent fission yield/temperature rise in Eq. (10). When the inertia effect is generated, there is no analytical solution for the relation between the reactivity change and displacement because the shape of the displacement distribution in the burst no longer remains the same as that in the static expansion case but changes over time. To obtain an accurate displacement or its distribution shape, neutronic–thermoelastic Eqs. (1)–(4) should be calculated, whereas in this coupled calculation, the unknown relation between the reactivity change and displacement should be first provided to develop the reactivity feedback model. To overcome this difficulty, the traditional method in early works simplified the elastic wave equation to obtain an approximate relation such as Eq. (11).

Considering all possible displacements in the burst can be expressed as the sum of a series of orthogonal functions, if the reactivity change component for the displacement in the form of each orthogonal function can be obtained, the total reactivity change can be obtained as the sum of all its components. The coefficient of the reactivity change component is the relative weight of the corresponding orthogonal function. However, this goal has never been achieved, because in early works the Monte Carlo codes were typically used to calculate the reactivity. The displacement in the burst is so small that the reactivity change may be of the same or of smaller magnitude as the calculation uncertainty [9]; the obtained relation between the reactivity change and displacement thus may be inaccurate or even incorrect. This difficulty can be overcome by using deterministic neutron transport codes such as the static neutron transport component of our FBR-MPC code. FBR-MPC is a 3D FEM multiphysical code for calculating the static neutronic field (mainly used as the initial condition for the burst simulation) and burst dynamic behavior in FBR by coupling the time-dependent neutron transport equations, heat conduction equation, and thermoelastic equations. Detailed information can be found in the literature [5].

Selecting the trigonometric functions as the orthogonal functions, the displacement at an arbitrary time can be expressed using the Fourier expansion method [12, 13] as follows:

$$u(r, t) = \frac{1}{2}a_0(t)w + \sum_{k=1}^K \left(a_k(t)w \sin\left(k \frac{2\pi r}{R'}\right) + b_k(t)w \cos\left(k \frac{2\pi r}{R'}\right) \right), \quad (18)$$

where a and b are the fitting coefficients, w is the small amplitude of trigonometric function, and $R' = R + \Delta r$, Δr is the discretized spatial distance.

Equation (18) can be rewritten in a matrix form as follows:

$$\mathbf{u} = \begin{bmatrix} u_1 \\ \vdots \\ u_R \end{bmatrix} = \mathbf{M}\mathbf{a} = \begin{bmatrix} w & w \sin \frac{2\pi r_1}{R'} & \cdots & w \cos \frac{2K\pi r_1}{R'} \\ \vdots & \vdots & \ddots & \vdots \\ w & w \sin \frac{2\pi R}{R'} & \cdots & w \cos \frac{2K\pi R}{R'} \end{bmatrix} \begin{bmatrix} a_0/2 \\ a_1 \\ \vdots \\ b_K \end{bmatrix}. \quad (19)$$

First, the reactivity of the unexpanded core is calculated. Thereafter, similar static calculations are performed for the expanded core with the displacement in the form of the

trigonometric function $\{w, w \sin(\frac{2\pi r}{R'}), \dots, w \cos(\frac{2K\pi r}{R'})\}$ in Eq. (18). The effect of displacement is considered by updating the node location in each FEM element with the displacement and recalculating the density in the reformed element based on the mass conservation law. Therefore, variations in macro-cross sections and neutron leakage area caused by the changes in material density and surface area can be determined. Once the reactivity change components $\Delta\rho_{\text{TR}}$ for all the displacements in the form of trigonometric functions are determined, the total reactivity change can be calculated as follows:

$$\Delta\rho(t) = (\mathbf{a}, \Delta\rho_{\text{TR}}) = (\mathbf{M}^{-1}\mathbf{u}, \Delta\rho_{\text{TR}}). \quad (20)$$

At each time step, after calculation of elastic wave Eq. (4), the coefficient array \mathbf{a} can be determined and the reactivity can be updated using Eqs. (12) and (20).

The Fourier expansion method, rather than the more widely used mode superposition method in mechanics, was used in this study. This is partly because for some FBRs, of which the mechanical property of the materials is sensitive to temperature change, the precalculated mode is unsuitable for calculating the displacement distribution during the entire burst. Another reason is that from the viewpoint of neutronics, the method applied in this study is much simpler and can be conveniently used in FBRs of different configurations; one does not need an expert-level knowledge of mechanics.

4 Results and discussion

4.1 Validation of the static neutron transport component of the FBR-MPC code

The static neutron transport calculation was performed for the spherical model of the Godiva reactor, and the calculated effective multiplication factor k_{eff} was 0.9978, very close to the measured 1.000 ± 0.001 [14] and 0.99629 ± 0.00009 obtained using the JMCT code [15]. Because of the lack of experimental data, the calculated neutron flux distribution was only compared to that obtained using JMCT as shown in Fig. 1. The two curves nearly overlap, indicating the validation of the static neutron transport component of the FBR-MPC code.

For the Godiva I reactor studied, with the application of the point kinetic approximation for neutronics and the adiabatic approximation for temperature, the fission rate and temperature rise in the burst have the same spatial distribution shape as the static neutron flux and can be expressed as a function in the form of $\sin(r/R'')/r$, where $R'' = 10.65$ cm is the extrapolation radius determined by the static neutron flux distribution calculated using the

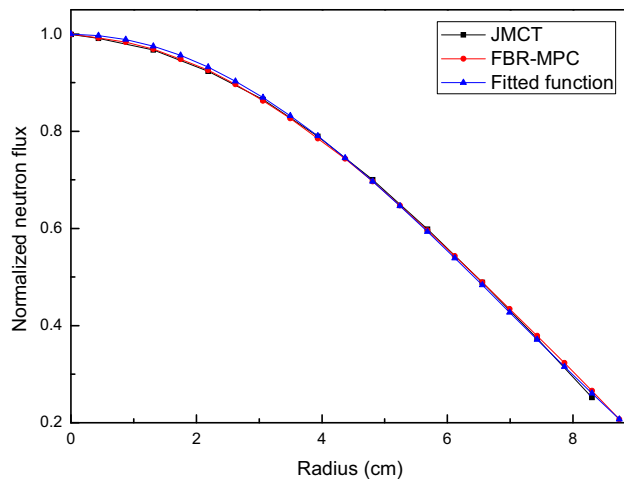


Fig. 1 Radial distribution of the normalized static neutron flux

FBR-MPC. The fitted function of $\sin(r/R'')/r$ is also shown in Fig. 1 and is consistent with the static neutron fluxes obtained using the FBR-MPC and JMCT codes.

4.2 Main burst parameters

Bursts triggered with different initial stepwise reactivities (0.65, 1.08, 2.09, 3.29, 5.99, and 8.37 ϕ above supercritical) were simulated using the simplified multiphysics models described in Sect. 2.1 and the displacement-reactivity feedback model described in Sect. 3. The results were compared to the experimental data and the solutions described in Sect. 2.4 using traditional fission yield (temperature rise)-reactivity feedback models described in Sect. 2.3.

As shown in Tables 2 and 3, for all selected bursts, the peak fission rates calculated using the developed displacement-reactivity feedback model and Eq. (13) using the experimental quench coefficient $b_f = 2.08\text{E}-17\text{ \$/f}$ correspond very closely to the values of the experimental data. In addition, for bursts with small initial reactivity (for instance $\rho_0 < 2.09\text{ }\phi$), the calculated fission yields are larger than the experimental yields, whereas the temperature rises are smaller than the experimental ones. This can be attributed to the heat capacity of the core employed in this study being higher than the realistic capacity. A larger heat capacity causes a smaller temperature rise and core expansion, and its induced reactivity feedback effect is consequently smaller than the experimental values. As a

result, the peak fission rate and fission yield tend to be overestimated.

For bursts with large initial reactivity (such as $\rho_0 = 8.37\text{ }\phi$), because the burst width in the traditional models remains the same as that upon neglecting the inertia effect (see Eq. (13)), the temporal integration of fission rate, i.e., the fission yield, is overestimated. It can thus be expected that the fission yield obtained using the displacement-reactivity feedback model will be closer to that obtained using the experimental data, because the smaller burst width and hence the smaller temporal integration of the fission rate caused by the inertia effect can be revealed. However, the calculated results deviate from the experimental data, as shown in Table 3. This deviation was also noticed in our previous work [5] and can be attributed to the neglect of the damping effect in Eq. (4). Notably, although the traditional models seem to provide more accurate results for fission yields for bursts with a large initial reactivity, they cannot reflect the realistic physical process of a burst because this coincidence is caused by the fact that the offsets of inertia and damping effects both lead to a small change in burst width. Moreover, the underestimation of fission yield results in a smaller temperature rise and surface displacement as compared to those of the experimental data and/or those obtained using Eqs. (16) and (17) with traditional models, as shown in Tables 4 and 5.

To obtain intuitive insight into the relation between the reactivity change and displacement, a new reactivity feedback coefficient b_s , defined as the absolute value of the reactivity change per unit change in surface displacement, is introduced, i.e., $b_s = |\Delta\rho|/u_R$.

For bursts with $\rho_0 \leq 2.09\text{ }\phi$, the results show that the inertia effect is not generated, i.e., the core expansion can accommodate the temperature rise, the shape of the displacement distribution remains the same as that in the case of static expansion, and only the magnitude of displacement changes. In such cases, b_s is equivalent to the quench coefficient b_f and they are in a linear relation of $b_f = \alpha_{fs}b_s$, $\alpha_{fs} = 6.02\text{E}-17\text{ cm/f}$ for the Godiva I reactor. As shown in Fig. 2, b_s remains constant at 36.21 $\text{\$/cm}$, corresponding to $b_f = 2.18\text{E}-17\text{ \$/f}$, very near the experimental value of $2.08\text{E}-17\text{ \$/f}$ [6].

As ρ_0 increases, a lag between the core expansion and temperature rise occurs because of the faster increase in the fission rate/power, the curve for the distribution shape of displacement is under those of bursts with $\rho_0 \leq 2.09\text{ }\phi$, and

Table 2 Peak fission rates for various bursts (s^{-1})

	0.65 ϕ	1.08 ϕ	2.09 ϕ	3.29 ϕ	5.99 ϕ	8.37 ϕ
Experiment	1.04E18	2.42E18	0.93E19	2.56E19	1.00E20	2.58E20
Equation (13)	1.04E18	2.88E18	1.08E19	2.95E19	1.18E20	2.83E20
This work	1.12E18	3.08E18	1.16E19	2.91E19	1.08E20	2.52E20

Table 3 Fission yields for various bursts

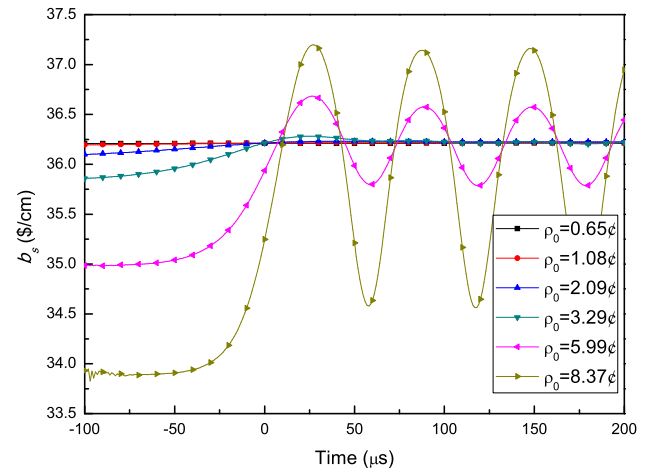
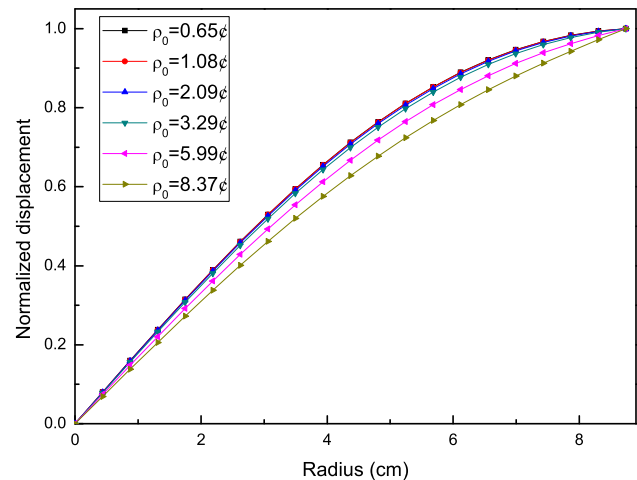
	0.65 ϕ	1.08 ϕ	2.09 ϕ	3.29 ϕ	5.99 ϕ	8.37 ϕ
Experiment	6.36E14	1.08E15	1.84E15	3.01E15	6.53E15	1.29E16
Equation (14)	6.23E14	1.04E15	2.01E15	3.48E15	7.64E15	1.31E16
This work	6.65E14	1.11E15	2.14E15	3.35E15	6.11E15	0.92E16

Table 4 Average temperature rises for various bursts (K)

	0.65 ϕ	1.08 ϕ	2.09 ϕ	3.29 ϕ	5.99 ϕ	8.37 ϕ
Experiment	3.24	5.51	9.39	15.36	36.10	65.83
Equation (16)	2.85	4.75	9.18	15.90	34.92	60.13
This work	3.04	5.05	9.78	15.32	27.95	42.19

the core appears to be compressed, as shown in Fig. 3. Thus, the application of Eq. (10) will underestimate both the peak fission rate and fission yield because the core expansion and its induced reactivity decrease are overestimated. To account for the inertia effect, early works modified the quench coefficient b_f such as in Eq. (11), whereas the modified quench coefficient b'_f remains constant, indicating that the shape of the displacement distribution remains the same as that in the bursts without an inertia effect, as shown in Eq. (17). This is in conflict with the fact that when the inertia effect is generated, the shape of the displacement distribution varies in the burst, as shown in Fig. 4. As a result, the impact of the variation in the distribution shape of the displacement on neutronics cannot be shown. Fortunately, this difficulty can be overcome using the developed displacement-reactivity feedback model.

As shown in Fig. 2, for bursts with $\rho_0 > 2.09 \phi$, at the initiation of the burst, because the fission power is very small, the temperature rise and its induced core expansion can be neglected. Thus, b_s remains practically constant. As the fission rate intensely increases, the temperature rise and core expansion vary sharply, leading to a rapid increase in b_s . Oscillations caused by the core vibration, noticed in other experiments [6, 7] and our previous work [5] but which cannot be reproduced using the traditional models, can be observed. Notably, for a burst with $\rho_0 = 3.29 \phi$, b_s finally does not tend to attain a constant value for the burst without an inertia effect but oscillates slightly with time because of the small inertia effect.

**Fig. 2** (Color figure online) Temporal variations in b_s for various bursts (0 represents time of t_{\max})**Fig. 3** (Color figure online) Radial distribution of normalized displacement during increasing periods of bursts

Moreover, using the displacement-reactivity feedback model, the more rapidly increasing velocity of the fission rate at the initiation of the burst, which has been noticed in the CFBR-II reactor [7] but cannot be reproduced using Eq. (13), can be observed. This is because the realistic

Table 5 Maximum surface displacements for various bursts (cm)

	0.65 ϕ	1.08 ϕ	2.09 ϕ	3.29 ϕ	5.99 ϕ	8.37 ϕ
Equation (17)	3.36E-4	5.60E-4	1.08E-3	1.88E-3	4.12E-3	7.09E-3
This work	3.59E-4	5.96E-4	1.15E-3	1.81E-3	3.37E-3	6.34E-3

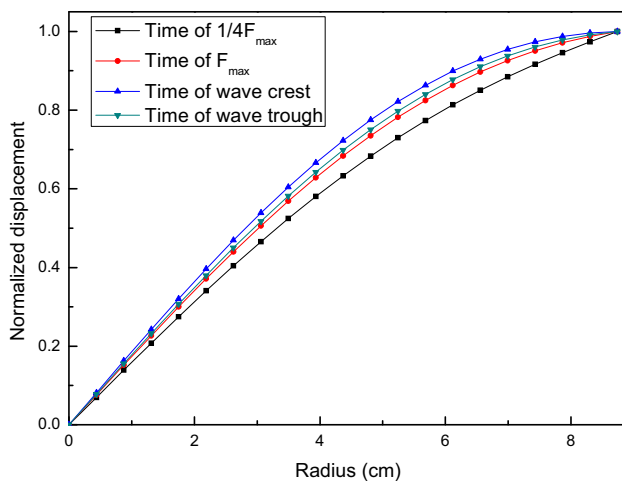


Fig. 4 (Color figure online) Radial distributions of normalized displacement for a burst with $\rho_0 = 8.37 \phi$

reactivity feedback coefficient b_s is smaller than b'_s (corresponding to b'_f in Eq. (11), forming a straight line below that for the burst with $\rho_0 \leq 2.09 \phi$ but still above the initial part of b_s in Fig. 2). In addition, during the drop period of the fission rate ($t > 0$ in Fig. 2), the larger b_s indicates a faster changing ratio of fission rate than during the increasing period ($t < 0$), leading to an asymmetry of the fission rate curve and smaller burst width (also see Fig. 6).

4.3 Temporal variations

Because of the lack of detailed experimental data, only the calculated temporal variations in reactivity, fission rate, average temperature rise, and surface displacement are presented and analyzed. The bursts with $\rho_0 \leq 1.08 \phi$ are not considered because in such cases these parameters are small (see Tables 2–5) and their temporal variations are very slow.

As shown in Figs. 5 and 6, for a burst without the inertia effect ($\rho_0 = 2.09 \phi$), the calculated results are similar to those obtained using Eqs. (10) and (13), i.e., the reactivity decreases from an initial value of ρ_0 to $-\rho_0$. This change is terminated during the drop period of the fission rate; the fission rate nearly increases/decreases in an exponential manner and its curve is symmetric about the peak.

For bursts with the inertia effect, the reactivity does not monotonically decrease to $-\rho_0$ as expected in early theoretical works [1], but a temporal oscillation is generated. For the bursts with $\rho_0 = 5.99 \phi$ and 8.37ϕ , the changing ranges of reactivity are $-6.00 \pm 1.20 \phi$ and $-9.74 \pm 5.51 \phi$, respectively, in the same period of core vibration (see Figs. 6 and 8). As the initial reactivity ρ_0 increases, the delay between the core expansion and temperature rise during the initial period of the burst becomes

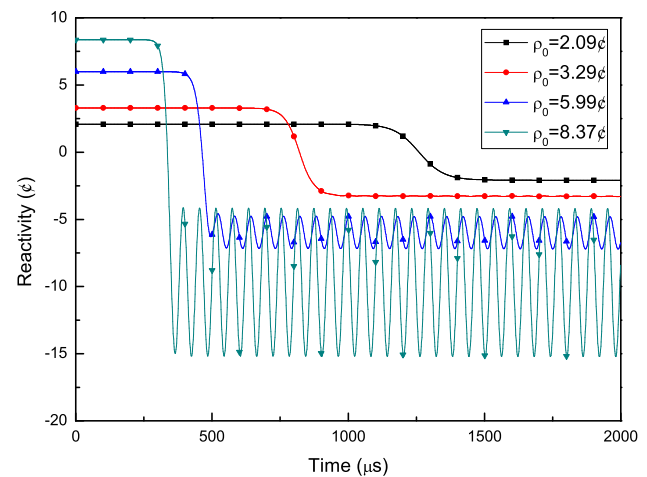


Fig. 5 (Color figure online) Temporal variations in the reactivity of various bursts

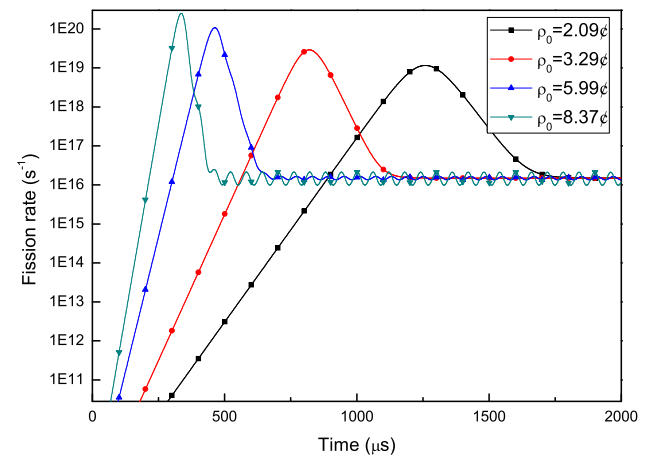


Fig. 6 (Color figure online) Temporal variations in the fission rate of various bursts

more significant (the smaller b_s in Fig. 2), which subsequently results in the more prominent core vibration and hence the larger oscillation amplitude of reactivity. In addition, the average reactivity is smaller than $-\rho_0$, which indicates that the FBR system will finally be in a deeper subcritical state rather than the recognized $-\rho_0$; this tendency is consistent with the experimental data of the CFBR-II reactor [7]. Moreover, because the reactor core changes from expansion to compression during the drop period of the burst (see Fig. 8), the reactivity changes from a decreased to an increased and the decreased ratio of the fission rate thus becomes smaller and the fission rate curve is distorted, as shown in Fig. 6. This tendency was first noticed in the literature [5] and was reconfirmed in this study.

The temporal variations in average temperature rises are shown in Fig. 7. The temperature sharply increases only when the fission rate (or the corresponding fission power) is

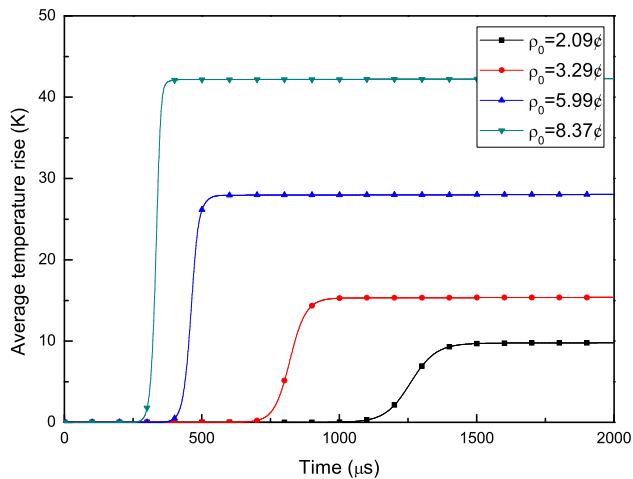


Fig. 7 (Color figure online) Temporal variations in the average temperature rise of various bursts

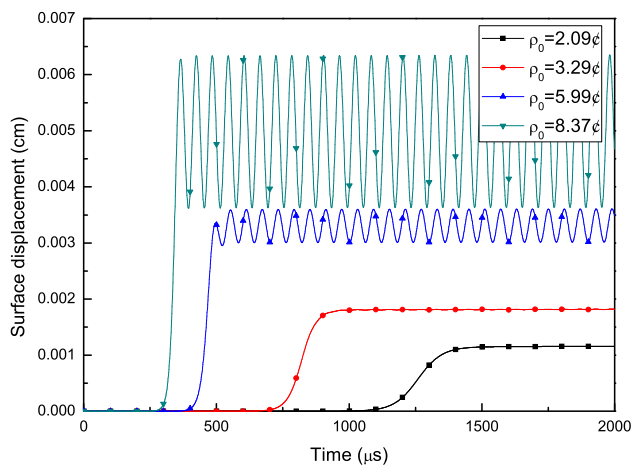


Fig. 8 Temporal variations in surface displacement for various bursts

sufficiently high ($F > 1\text{E}17/\text{s}$). At the beginning of the plateau following the burst, the fission power (the corresponding fission rate is in the magnitude of $1\text{E}16/\text{s}$, see Fig. 6) is much larger than the heat loss ratio through the core surface given the heat transfer and thermal radiation effects. Therefore, the temperature rises at a very slow rate. Notably, if the reactor core is not scrammed, for bursts with a prominent inertia effect, the increasing temperature will lead to a stronger core vibration and the stress also increases and may exceed the yield strength, resulting in material failure.

For a burst without the inertia effect ($\rho_0 = 2.09\text{ ¢}$), the core expansion can accommodate the temperature rise and the displacement at an arbitrary position of the core increases in the same manner as expected using Eq. (7). The surface displacement monotonically increases and tends to a constant value such as that in the static expansion, whereas for a burst with the inertia effect, the core

finally converts to an undamped free vibration, and the vibration amplitude increases for bursts with a larger initial reactivity, as shown in Fig. 8. The calculated vibration period is $60\text{ }\mu\text{s}$, consistent with that obtained performing an accurate 3D dynamic coupled multiphysical simulation using the FBR-MPC code [5]. Because of the underestimation of fission yield for a burst with $\rho_0 = 8.37\text{ ¢}$ using the developed displacement-reactivity feedback model, the calculated maximal equivalent stress is $\sim 121\text{ MPa}$ on the core surface, smaller than that obtained using the dynamic simulation of the FBR-MPC code.

5 Conclusion

This study developed a displacement-reactivity feedback model applicable to all bursts by establishing the relation between the reactivity change and displacement with the aid of the static neutron transport component of the FBR-MPC code. Coupled simulations using this developed model and simplified multiphysics models were performed for various bursts in the Godiva I reactor. The results were compared to the experimental data and those obtained using traditional fission yield (temperature rise)-reactivity feedback models.

It was found that similar to traditional models, the developed displacement-reactivity feedback model can provide good results for bursts with no or a small inertia effect. For bursts in which the inertia effect is prominent, although the calculated results deviate from the experimental data because of the assumption of undamped free core vibration, the smaller burst width and asymmetric distribution of the fission rate curve, noticed in experiments but which cannot be reproduced using traditional models, can be shown. In addition, the realistic reactivity and fission rate oscillations caused by the core vibration, as well as the deeper sub-prompt criticality in the plateau following the burst, can be observed. Therefore, the developed displacement-reactivity feedback model can be expected to be an effective tool for simulating burst dynamic behavior.

References

1. R.F. He, M.C. Deng, *Experiments and Physics on Fast-Neutron Critical Facilities and Pulsed Reactors* (National Defense Industry Press, Beijing, 2012), p. 422
2. E.P. Shabalin (ed.), *Fast Pulsed and Burst Reactors* (Pergamon Press, New York, 1979)
3. T.J. Grove, R.H. Kimpland, W.L. Myers, A dynamic simulation tool for critical assemblies using the coupled neutronic-thermoelastic method, *Paper presented at the American Nuclear Society 2008 Winter Meeting, Reno, Nov 2008*, pp. 9–13

4. C. Fiorina, M. Auferio, S. Pelloni, et al., A time-dependent solver for coupled neutron transport thermal-mechanics calculations and simulation of a Godiva prompt-critical burst. ASME. *International Conference on Nuclear Engineering, Volume 4: Radiation Protection and Nuclear Technology Applications; Fuel Cycle, Radioactive Waste Management and Decommissioning; Computational Fluid Dynamics (CFD) and Coupled Codes; Reactor Physics and Transport Theory*: V004T11A008. Prague, Czech Republic, July 7–11, 2014. <https://doi.org/10.1115/icon22-30395>
5. J. Wang, W.F. Liang, S. Chen et al., Dynamic behavior in fast burst reactor with three-dimensional coupled multiphysics method. *Nucl. Eng. Des.* **338**, 16–22 (2018). <https://doi.org/10.1016/j.nucengdes.2018.07.026>
6. T.F. Wimett, Time Behavior of Godiva Through Prompt Critical (Los Alamos National Laboratory Web, 1995). <https://fas.org/sgp/othergov/doe/lanl/lib-www/la-pubs>. Accessed 28 July 1995
7. J. Li, H. Gao, M. Li et al., Analysis of shutdown physics progress of CFBR-II. *Atom. Energy Sci. Technol.* **47**(3), 355–358 (2013). <https://doi.org/10.7538/yzk.2013.47.03.0355>. (in Chinese)
8. W.Z. Chen, L.F. Guo, B. Zhu et al., Accuracy of analytical methods for obtaining supercritical transients with temperature feedback. *Prog. Nucl. Energy* **49**, 290–302 (2007). <https://doi.org/10.1016/j.pnucene.2007.01.004>
9. S.C. Wilson, S.R. Biegalski, R.L. Coats, Computational modeling of coupled thermomechanical and neutron transport behavior in a Godiva-like nuclear assembly. *Nucl. Sci. Eng.* **157**, 344–353 (2007). <https://doi.org/10.13182/NSE06-28>
10. G.I. Bell, S. Glasstone, *Nuclear Reactor Theory* (van Nostrand Reinhold Company, New York, 1970), p. 54
11. S.Y. Kadioglu, D.A. Knoll, Multiphysics analysis of spherical fast burst reactors. *Nucl. Sci. Eng.* **163**, 132–143 (2009). <https://doi.org/10.13182/NSE09-07>
12. W.R. Stratton, Analysis of prompt excursions in the simple systems on idealized fast reactors, *Paper presented at the international conference on the peaceful uses of atomic energy*, Geneva, Sep 1958, pp. 1–13
13. Q.Y. Li, N.C. Wang, D.Y. Yi, *Numerical Analysis*, 3rd edn. (Tsinghua University Express, Beijing, 2015), p. 51
14. R.J. LaBauve (ed.), *International Handbook of Evaluated Criticality Safety Benchmark Experiments* (Nuclear Energy Agency, Paris, 2003)
15. G. Li, B.Y. Zhang, L. Deng et al., Development of Monte Carlo particle transport code JMCT. *High Power Laser Part. Beams* **25**(01), 158–161 (2013). <https://doi.org/10.3788/HPLPB20132501.158>. (in Chinese)